A Semicircular Substrate Integrated Waveguide-Based Self-Diplexing Slot Antenna With Polarization Flexibility

Meha Agrawal, *Student Member, IEEE*, and Trivesh Kumar, *Member, IEEE*

***Abstract*—The substrate integrated waveguide (SIW) based self-diplexing antenna having polarization flexibility is presented in this letter for satellite communications. The presented self-diplexing antenna can provide the linear polarization, right-hand circular polarization, and left-hand circular polarization at the two closely spaced frequencies with the respective port. The antenna is realized on a semicircular SIW cavity, which is further modified to form the two dominant mode quadrant cavities by incorporating a via wall at the center of the semicircular cavity. The different polarizations are achieved by changing the orientation of the radiating slots. The linear polarization is achieved by loading the curved slots in a back-to-back manner and circular polarization in a crossed manner. The resonant frequencies can be tuned with the help of the length of the slots. The equivalent circuit model of the proposed antenna is developed and the equivalent parameters are extracted. The testing of two fabricated antenna prototypes with different polarizations is presented here.**

***Index Terms*—Cavity-backed antenna, circularly polarized (CP), patch, substrate integrated waveguide (SIW) antenna, wideband.**

I. Introduction

The satellite communication systems largely demand low-profile dual-frequency antennas [1], [2]. Usually, dual-frequency antennas are designed to operate on a single feed structure [3]. However, to select the required frequency band, self-diplexing antennas emerged to provide isolation between the two frequencies and to reduce the overall size, weight, and complexity of these dual-frequency antennas. The challenges associated with self-diplexing antennas are to improve the gain, power handling capability, polarization flexibility, and front-to-back ratio (FTBR) [4]. The substrate integrated waveguide (SIW) technology has recently emerged and can be efficiently utilized to design low profile, high gain, size miniaturization, and unidirectional planar antennas [5], [6], [7]. The electric field also remains confined between the via walls, therefore it provides good isolation as well as easy integration with other planar circuits. Several geometries have been proposed for self-diplexing antennas, like bow tie slot [8], two dissimilar U-shaped slots, and two dissimilar transverse slots [9], [10] excited by two transverse microstrip feed lines; however, all reported similar linear polarization for both the ports. For the enhancement of the isolation, the utilization of the via wall along with the slots has been reported in [11]. A rectangular ring-shaped slot with microstrip feeds in [12] and [13] is utilized for achieving dual-band orthogonal polarization with size compactness. In [14], two dissimilar orthogonal rectangular slots are excited using transverse microstrip feedlines to achieve circular polarization.

In this letter, an SIW-based self-diplexing antenna with polarization flexibility is presented. The two antenna variants are fabricated and tested for a different set of polarizations. The antenna structure is designed by utilizing the TE_{120} mode of the semicircular SIW cavity. The semicircular SIW cavity is split into two separate dominant mode quadrant cavities (DMQC) by placing a via wall at the position of the electric wall in the center of the cavity. Each DMQC is loaded with a pair of curved slots. The slots are arranged in a back-to-back manner for linear polarization and in a cross manner for circular polarization. An equivalent circuit model is also developed with the detailed parametric validation of the antenna design. The proposed antenna can be efficiently utilized for various satellite applications with desired polarizations.

II. Antenna Configuration

The design configurations of the proposed semicircular SIW cavity-based self-diplexing antenna with two different polarizations are depicted in Fig. 1. The broadside linearly polarized radiation is achieved by incorporating the back-to-back connected two pairs of thin elliptical curved-shaped slots on the top layer of the cavity (Antenna-1). For the circularly polarized (CP) radiation, the cross-shaped curved slots are utilized (Antenna-2). The dimensions of the semicircular SIW cavity and inset microstrip feed are kept identical for all three antenna variants.

A. Antenna Design and Analysis

The dimensions of the cavity are chosen according to the predefined rules [15], [16] such that the antenna operates in X-band. The eigen mode TE_{120} exists inside the cavity at the frequency of 11.5 GHz. Two pairs of back-to-back connected elliptical curve-shaped slots are loaded on the cavity at the position of the maximum electric field corresponding to TE_{120} mode.

The minor and major radii r_{nij} and r_{mij} ($i_{\text{ ports}} = 12$ and $j_{\text{antennas}} = 12$) of the curved slot govern the curved length of the slot. Thus, the curved length of slots at port-1 and port-2 is set at the values 9.15 and 8.93 mm, respectively, such that antennas

Manuscript received 1 February 2023; accepted 19 February 2023. Date of publication 27 February 2023; date of current version 7 July 2023. This work was supported by the Indian Institute of Information Technology, Design, and Manufacturing, Jabalpur, Madhya Pradesh, India. *(Corresponding author: Trivesh Kumar.)*

The authors are with the Department of Electronics Engineering, Indian Institute of Information Technology Design and Manufacturing, Jabalpur 482005, India (e-mail: 1822604@iiitdmj.ac.in; trivesh@iiitdmj.ac.in).

Digital Object Identifier 10.1109/LAWP.2023.3249350

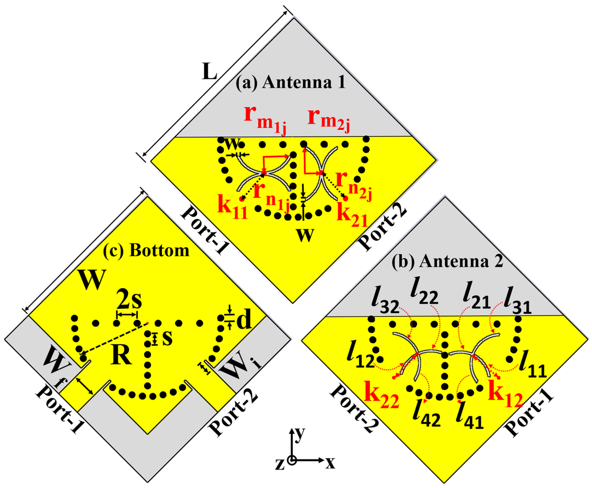

Fig. 1. Geometrical configuration of the proposed semicircular SIW cavity-based self-diplexing antennas.

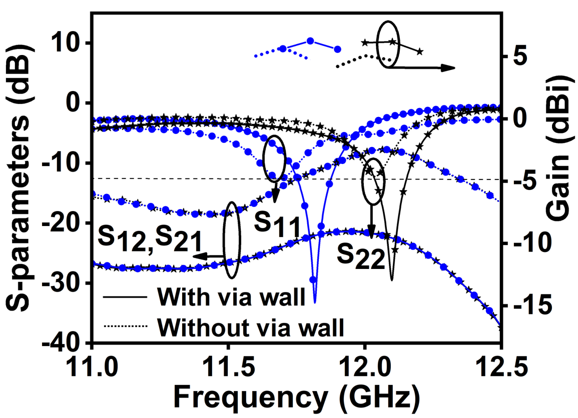

Fig. 2. S-parameters of Antenna 1 with and without via wall inside the semi circular SIW cavity.

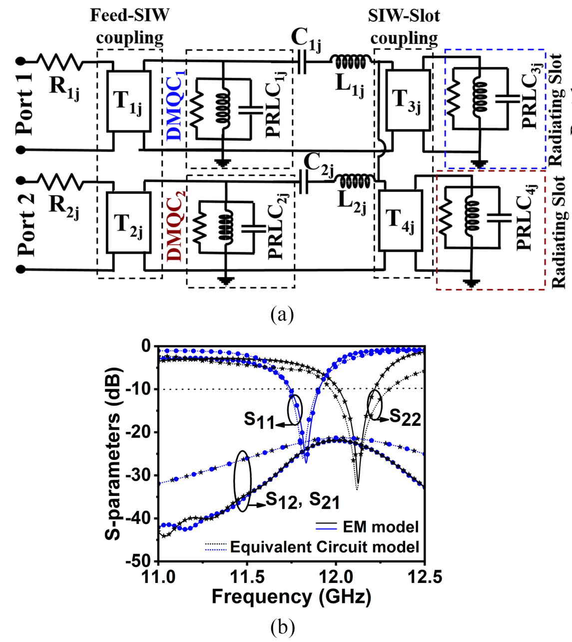

Fig. 3. (a) Equivalent circuit model of the proposed antenna. (b) Simulated *S*-parameters of EM model and ECM model of Antenna 1.

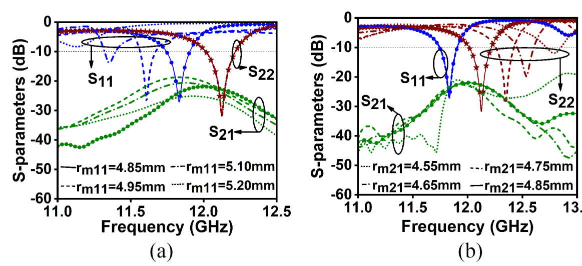

Fig. 4. Effect of variation of major radius of the slots at (a) port-1 and (b) port-2 of Antenna-1.

radiate at desired frequencies. The orientation of both the slot pairs is kept orthogonal, which eventually produces orthogonal linear polarization. Further, to improve the isolation between the two ports, extra metallic vias (via wall) are placed at minimum electric field position at the center of the SIW cavity along the y-axis. This arrangement splits the semicircular SIW cavity into two equivalent quadrants leading to the formation of the two DMQCs. The linearly polarized self-diplexing antenna structure is shown in Fig. 1(a) corresponding to Antenna-1. The optimized dimensions are $L = 34$, $W = 28$, $W_f = 4.74$, $W_i = 3$, $R = 13$, $d = 1$, $S = 1.85$, $w = 0.5$, $k_{11} = 6.15$, $k_{21} = 6.05$, $r_{m11} = 4.85$, $r_{m21} = 4.85$, $r_{n11} = 3.3$, and $r_{n21} = 2.8$. The improvement in inter port isolation from 8 to 20 dB by introducing via wall is observed by studying the S_{11}, S_{22}, and S_{21} of Antenna-1 as shown in Fig. 2. The substantial enhancement in the gain and S_{11} bandwidth is also observed with the small shift in the two resonant frequencies.

B. Equivalent Circuit Model

The equivalent circuit model of the proposed self-diplexing antenna is developed and depicted in Fig. 3(a). This circuit model is applicable to all the polarization variants; however, the circuit element values will be different. The circuit element values for Antennas 1 and 2 are discussed. The circuit components parallel-connected *RLC* ($PRLC_{1j}$ and $PRLC_{2j}$) (j = Antennas-12) represent the individual DMQC resonance modes. The coupling between these DMQCs and microstrip feed is modeled by the transformers T_{1j} and T_{2j}. The curved slots are modeled by the components $PRLC_{3j}$ and $PRLC_{4j}$ for port-1 and port-2, respectively. The coupling between the slots at port-1 and port-2 and the SIW cavity is modeled by the ideal transformers T_{3j} and T_{4j}. The loading effect in the individual DMQC is represented by series L_{ij} C_{ij} (i = ports 12) components. The two microstrip feedlines are represented by R_{1j} and R_{2j}. The circuit is simulated and optimized using Keysight ADS software. The comparison of response of Antenna 1 obtained from the equivalent circuit and full-wave electromagnetic (EM) simulation is shown in Fig. 3(b). The circuit element values for Antenna-1 are $R_{11} = 4.65\ \Omega$; $R_{21} = 4.16\ \Omega$; $T_{11} = 1.9$; $T_{21} = 1.79$; $PRLC_{11} = 2.93$ KΩ, 0.36 nH, 1.044 pF; $PRLC_{21} = 0.18$ KΩ, 0.43 nH, 0.62 pF; $C_{11} = 0.2$ pF, $L_{11} = 1.22$ nH; $C_{21} = 0.2$ pF, $L_{21} = 1.57$ nH; $T_{31} = 1.96$; $T_{41} = 1.96$; $PRLC_{31} = 4.48$ KΩ, 0.51 nH, 0.14 pF; $PRLC_{41} = 4.22$ KΩ, 2.23 nH, 0.19 pF.

TABLE I
EFFECT OF VARIATION OF CURVED SLOT LENGTH AT PORT-1

Reso. freq. (GHz)	Circuit model		Curved slot length (port-1) (mm)
	C_{31}=0.1457 pF (fixed)	L_{31}=0.512 nH (fixed)	
	L_{31} (nH)	C_{31} (pF)	
11.12	1.862	0.1857	13.4
11.37	1.742	0.1689	13.2
11.61	1.622	0.1557	12.9
11.87	0.512	0.1457	12.5

Effect of variation of curved slot length at port-2

Reso. freq. (GHz)	Circuit Model		Curved slot length (port-2) (mm)
	C_{41}=0.1994 pF (fixed)	L_{41}=2.236 nH (fixed)	
	L_{41} (nH)	C_{41} (pF)	
12.1	2.2368	0.1994	12.3
12.25	2.3381	0.1745	12.2
12.5	2.4378	0.1545	12.0
12.75	2.5381	0.1405	11.75

TABLE II
VARIOUS POLARIZATION STATES OF ANTENNAS 1 AND 2

Slot rotation @Port-1	Slot rotation @Port-2	Port-1	Port-2	Antenna structure
0° with respect to feed (normal to the feed)				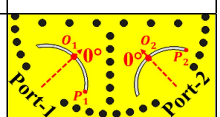
45° anticlockwise	45° anticlockwise	Orthogonal linear polarization [Antenna 1]		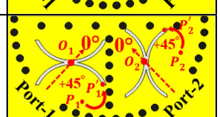
45° anticlockwise	45° clockwise	Same linear polarization [other pol. states]		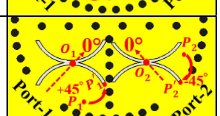
20° anticlockwise, 60° clockwise	20° clockwise, 60° anticlockwise	LHCP	RHCP	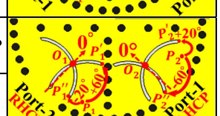
		[Antenna 2]		
20° anticlockwise, 60° clockwise	20° anticlockwise, 60° clockwise	LHCP	LHCP	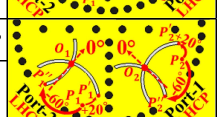
		[other pol. states]		
20° clockwise, 60° anticlockwise	20° clockwise, 60° anticlockwise	RHCP	RHCP	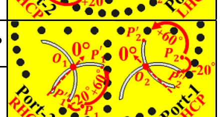
		[other pol. states]		
20° clockwise, 60° anticlockwise	20° anticlockwise, 60° clockwise	RHCP	LHCP	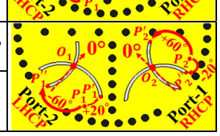
		[other pol. states]		

C. Parametric Analysis

The variation in each curved slot length is achieved by the variation of the major radii (r_{mij}) or minor (r_{nij}). Fig. 4(a) and (b) shows the effect of variation in the major radius r_{m11} at port-1 and r_{m21} at port-2, respectively. An increase in the major radius of back-to-back connected slots at port-1 increases the curved slot length thereby shifting the resonant frequency of port-1 toward the lower frequency regime. These major radii can be varied from 4.85 to 5.10 mm to get a wider tuning range of lower resonant frequency with good isolation as shown in Fig. 4(a).

TABLE III
MEASURED PERFORMANCE PARAMETERS OF ANTENNAS 1 AND 2

Antenna	Port	Freq. (GHz)	IBW (GHz)	ARBW (GHz)	Gain (dB)	Isolation (dB)	Pol.
Antenna-1	Port-1	11.87	11.70–11.93	N.A.	6.09	22.7	Ortho-LP
	Port-2	12.1	11.95–12.26	N.A.	5.87	22.5	
Antenna-2	Port-1	11.35	11.25–11.45	11.3–11.42	5.24	27.3	Ortho-CP
	Port-2	11.92	11.80–11.97	11.8–11.97	5.11	24.2	

N.A. (not applicable); LP– linear polarization; CP– circular polarization

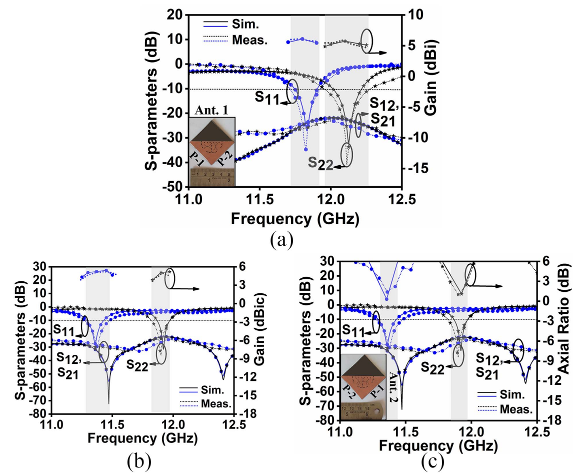

Fig. 5. Measured and simulated performance of antennas with (a) linear polarization (Antenna-1), and (b) and (c) orthogonal CP (Antenna-2).

Similarly, Fig. 4(b) depicts the tuning range of higher resonant frequency from 12.1 to 12.8 GHz by varying the r_{m21} from 4.85 to 4.55 mm. A similar effect of the shift in the resonant frequency at port-1 and port-2 can also be achieved by varying minor radii of back-to-back connected curved slots of each DMQC. The equivalent circuit element values corresponding to the variation of major and minor radii of the curved slots are shown in Table I.

III. CIRCULARLY POLARIZED SELF-DIPLEXING ANTENNA

The configuration of the CP self-diplexing antenna is shown in Fig. 1(b). Two dissimilar length curved slots in a cross pattern are etched on the top of each DMQC to obtain the CP radiation for both ports. The design methodology is similar to that discussed in Section II. The DMQC loaded with the cross-curved slots produces the orthogonal degenerate modes by a single feed. The angle between the cross-curved slot and the length of each slot is adjusted to achieve the CP at the desired resonant frequency. The resonant frequencies are controlled by varying the curved slot lengths similar to Antenna 1. However, in CP configuration (Antenna-2), the working frequencies can be shifted only toward the higher frequency regime by simultaneously decreasing the lengths (l_{32} and l_{22}) for port-2 and (l_{21} and l_{31}) for port-1. Shifting the frequencies toward the lower frequency regime disturbs the impedance matching and also affects the axial ratio. The impedance matching for a good axial ratio is also controlled by fixing the distance between the center of the slots and the microstrip line (k_{13}, k_{23}). The overall frequency ratio of 1.05–1.079 is obtained with an axial ratio below 3 dB and a minimum of 20 dB isolation. The resonant frequencies of Antenna-2 are 11.35 and 11.92 GHz. The dimensions of Antenna-2 are $l_{11} = 5.5$, $l_{21} = 4.75$, $l_{31} = 6.7$, $l_{41} = 5.5$, $l_{12} =$

TABLE IV
COMPARISON OF ANTENNAS 1 AND 2 WITH LITERATURE

Ref.	Freq. (GHz)	FTBR (dB)	X-pol. (dB)	Gain (dB)	Pol.	Isolation (dB)	Size (λ_0^2)	PF
[8]	8.9, 11.3	>19	19, 13	4.3, 4.2	LP	25	0.4	No
[10]	8.2, 10.4	23, 20	22, 20	3.5, 5.2	LP	29.7	0.3	No
[12]	9.5, 10.5	N.A.	24	5.7, 5.9	LP	24.0	0.4	No
[17]	9.8, 11.6	N.A.	22.0	7.0, 8.4	LP	20.5	1.4	No
[14]	11.2,11.7	15.2, 14.1	27, 25	5.8, 4.7	LP	17.8, 20.4	0.24	CP
	11.7, 12.3	15.2, 16.9	23,27	5.6, 5.9	LP	18.5, 14.0	0.27	CP
This work	11.8, 12.1	15.0, 15.2	25, 19	6.09, 5.87	LP	22.7, 22.5	0.38	Both CP and LP
	11.3, 12.1	19.8,15.1	20,20	5.24, 5.11	CP	27.3, 24.2		

PF: Polarization flexible

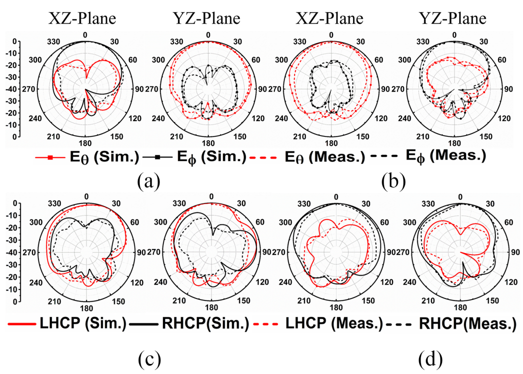

Fig. 6. Measured and simulated radiation pattern of Antenna 1 at (a) 11.87 and (b) 12.1 GHz; Antenna 2 at (c) 11.35 and (d) 11.92 GHz.

5.25, $l_{22} = 4.49$, $l_{32} = 6.55$, $l_{42} = 5.25$, $k_{12} = 6.05$, $k_{22} = 5.95$, $r_{m12} = 4.85$, $r_{m22} = 4.85$, $r_{n12} = 3.3$, and $r_{n22} = 2.8$. (all units in mm). The values of equivalent-circuit elements are $R_{12} = 3.79$ Ω; $R_{22} = 3.37$ Ω; $T_{12} = 1.9$; $T_{22} = 1.79$; PRLC$_{12}$ = 6.8 KΩ, 0.35 nH, 1.05 pF; PRLC$_{22}$ = 0.166 KΩ, 0.42 nH, 0.63 pF; C_{12} = 0.19 pF, L_{12} = 1.22 nH; C_{22} = 0.2 pF, L_{22} = 1.72 nH; PRLC$_{41}$ = 5.72 KΩ, 2.4 nH, 0.11 pF. The other possible combinations of polarization are shown in Table II. These are possible by choosing the desired orientation of curved slots at each port, respectively.

IV. Antenna Fabrication and Measurement

The two antenna structures are fabricated on a 1.57 mm thick Rogers RT/Duroid 5870 substrate using an LPKF Protomat S103 machine. The measurement of the *S*-parameters, gain, and axial ratio of the fabricated antennas is performed and the comparison between the simulated and measured results is depicted in Fig. 5(a)–(c). The measured isolation and gain are more than 20 and 5.0 dB, respectively, for both the fabricated antennas. The measured and simulated radiation patterns of the fabricated antennas at both the ports in the *XZ*-plane and the *YZ*-plane are shown in Fig. 6(a)–(d). Both antennas exhibit unidirectional radiation pattern with cross polarization below −15 dB in the broad side direction. Antenna-1 exhibits linear polarization at the two ports, and Antenna-2 exhibits LHCP at port-1 and RHCP at port-2. The measurement results of antenna prototypes in terms of gain, bandwidth, isolation, and polarization are summarized in Table III. The performance comparison of the proposed antennas in terms of FTBR, gain, and isolation is performed with those available in the literature and shown in Table IV. It can be observed from the comparison that the proposed low-profile antenna is the only self-diplexing antenna with the feature of polarization flexibility.

V. Conclusion

The novel design of a polarization flexible SIW-based self-diplexing antenna is presented in this letter. The antenna design is capable of providing any set of polarization at two frequencies. Each DMQC is loaded with curved slots and fed by an inset-microstripline. Two antenna variants with different sets of polarizations are fabricated and tested. A good correlation between the measured and simulated results is observed. The equivalent circuit model also validates the working of all the antenna structures. Along with the enhanced gain, good isolation, and FTBR, the proposed self-diplexing antenna is having the advantage of polarization flexibility, suitable for X- and Ku-band satellite applications.

References

[1] S. H. S. Esfahlani, A. Tavakoli, and P. Dehkhoda, “A compact single-layer dual-band microstrip antenna for satellite applications,” *IEEE Antennas Wireless Propag. Lett.*, vol. 10, pp. 931–934, 2011.
[2] A. A. Omar, M. C. Scardelletti, Z. M. Hejazi, and N. Dib, “Design and measurement of self-matched dual-frequency coplanar waveguide-fed-slot antennas,” *IEEE Trans. Antennas Propag.*, vol. 55, no. 1, pp. 223–226, Jan. 2007.
[3] X. Bao and M. J. Ammann, “Dual-frequency dual-sense circularly-polarized slot antenna fed by microstrip line,” *IEEE Trans. Antennas Propag.*, vol. 56, no. 3, pp. 645–649, Mar. 2008.
[4] M. Agrawal and T. Kumar, “A substrate integrated waveguide (SIW) based self-quadruplexing antenna for Ku-band applications,” *Int. J. Microw. Wireless Technol.*, pp. 1–9, 2022, doi: 10.1017/S1759078722000265.
[5] F. Xu and K. Wu, “Guided-wave and leakage characteristics of substrate integrated waveguide,” *IEEE Trans. Microw. Theory Techn.*, vol. 53, no. 1, pp. 66–73, Jan. 2005.
[6] D. Deslandes and K. Wu, “Accurate modeling, wave mechanisms, and design considerations of a substrate integrated waveguide,” *IEEE Trans. Microw. Theory Techn.*, vol. 54, no. 6, pp. 2516–2526, Jun. 2006.
[7] Q. Lai, C. Fumeaux, W. Hong, and R. Vahldieck, “Characterization of the propagation properties of the half-mode substrate integrated waveguide,” *IEEE Trans. Microw. Theory Techn.*, vol. 57, no. 8, pp. 1996–2004, Aug. 2009.
[8] S. Mukherjee and A. Biswas, “Design of self-diplexing substrate integrated waveguide cavity-backed slot antenna,” *IEEE Antennas Wireless Propag. Lett.*, vol. 15, pp. 1775–1778, 2016.
[9] A. Boukarkar, X. Q. Lin, Y. Jiang, and Y. Q. Yu, “A tunable dual-fed self-diplexing patch antenna,” *IEEE Trans. Antennas Propag.*, vol. 65, no. 6, pp. 2874–2879, Jun. 2017.
[10] S. Nandi and A. Mohan, “An SIW cavity-backed self-diplexing antenna,” *IEEE Antennas Wireless Propag. Lett.*, vol. 16, pp. 2708–2711, 2017.
[11] M. Agrawal and T. Kumar, “Wideband SIW based self-diplexing antenna using parasitic slots,” in *Proc. 2nd Int. Conf. Electron. Sustain. Commun. Syst.*, 2021, pp. 649–652.
[12] A. A. Khan and M. K. Mandal, “Compact self-diplexing antenna using dual-mode SIW square cavity,” *IEEE Antennas Wireless Propag. Lett.*, vol. 18, pp. 343–347, 2019.
[13] M. Agrawal and T. Kumar, “SIW-based enhanced gain self-diplexing antenna using higher order modes,” *J. Electromagn. Waves Appl.*, vol. 36, no. 7, pp. 1–16, 2021.
[14] S. Priya, K. Kumar, S. Dwari, and M. K. Mandal, “Circularly polarized self-diplexing SIW cavity backed slot antennas,” *IEEE Trans. Antennas Propag.*, vol. 68, no. 3, pp. 2387–2392, Mar. 2020.
[15] T. Hong, Z. Zhao, W. Jiang, S. Xia, Y. Liu, and S. Gong, “Dual-band SIW cavity-backed slot array using TM020 and TM120 modes for 5G applications,” *IEEE Trans. Antennas Propag.*, vol. 67, no. 5, pp. 3490–3495, May 2019.
[16] D. M. Pozar, *Microwave Engineering*. Hoboken, NJ, USA: Wiley, 2011.
[17] S. Priya, K. Kumar, S. Dwari, and M. K. Mandal, “Wideband SIW self-diplexing antenna with simultaneous control of bandwidth and band position,” *AEU-Int. J. Electron. Commun.*, vol. 138, 2021, Art. no. 153877.